International Journal of Electrical Engineering and Sustainability (IJEES)
ISSN (online): 2959-9229
https://ijees.org/index.php/ijees/index
Arab Impact Factor: 1.51
Volume 4 | Number 1 | January-June 2026 | Pages 85-102

An Integrated PLL–LCL–VSG Framework for Improving Grid Synchronization and Power Quality in Multi-Inverter Photovoltaic Power Plants

Khakim Muratov[1], Kamoliddin Kadirov[2*], Khusniya Ibragimova[3], Alijon Kushev[4], Khulkaroy Yusupaliyeva[5], Alisher To‘xtashev[6]

[1,2,4,5]The institute of energy problems of the academy of Sciences of the Republic of Uzbekistan, Tashkent, Uzbekistan
[3]Navoi State University of Mining and Technologies, Navoi, Uzbekistan
[6]Fergana State Technical University

[*]Corresponding author: kamoliddin.8484@mail.ru

Received: March 05, 2026 Accepted: May 25, 2026 Published: June 21, 2026
DOI:10.65998/ijees.v4i1.165

Abstract: The penetration of PV power plants into modern power grids requires an integrated, coherent and reliable control architecture for inverters that is able to maintain the synchronization, frequency, and power quality with dynamic operations. In this work, we propose a PLL-LCL-VSG control architecture for grid-connected PV inverters that are used at peak-load times. Our system is a phase-locked loop (PLL) that synchronizes grids as per the standard, LCL filter to attenuate the harmonic, and a VSG controller to handle the frequency and virtual inertia. We developed a detailed MATLAB/Simulink model to measure the dynamic performance of our proposed control architecture for different load scenarios. The results of the simulation showed the correct synchronization with the RMS phase error of 0.19381° and phase-error settling time of 0.02355 s. The frequency was within the range 49.903 - 50.093 Hz with the maximum absolute frequency deviation of 0.097406 Hz. Harmonic analysis has shown that the THD reduces from 42.539% to 1.9054% (95.521% in the case of current THD) with the current THD decreasing by 22.691%. The inverter successfully provided 150 kW peak load with dynamic settling time of 0.085145 s and reactive power support up to 32.788 kVAr. The results indicate that the proposed PLL-LCL-VSG architecture increases the synchronization accuracy, frequency regulation capability, harmonic suppression and peak-load support performance. Thus, the proposed framework is a promising model to improve the stability and power quality of grid-connected photovoltaic generation plants during peak electricity demand.

Keywords: Photovoltaic inverter, Virtual synchronous generator, VSG control, Phase-locked loop, PLL synchronization, ,Harmonic mitigation, Power quality.

1. Introduction

The rapid development of renewable energy sources and the development of PV generation systems for electric power systems have transformed the operational characteristics of current power systems [1]. For many countries, large scale solar power plants are also essential for energy transition strategies aimed at reducing greenhouse gas emissions and improving energy security [2]. However, the increase in inverter-based renewable generation has brought new challenges for grid stability, synchronization accuracy, power quality and frequency regulation, especially during periods of peak electricity demand.

Unlike conventional synchronous generators, photovoltaic power plants are connected to the electrical grid by power electronic converters. Consequently, the dynamics of the entire generating system is highly dependent on inverter control strategies and synchronization algorithms [3].

During peak load periods, the power system is subject to rapid load variations, voltage fluctuations, harmonic distortion and frequency deviation, which may negatively impact the synchronization performance of grid connected PV inverters [4]. When this happens, the phase angle error, the total harmonic distortion (THD), the power oscillation, the power quality and even the instability of the connected renewable energy systems may be adversely affected. Many synchronization algorithms based on Phase-Locked Loop (PLL) algorithms have been proposed to guarantee dependable grid integration and have been extensively studied [5]. The traditional Synchronous Reference Frame PLL (SRF-PLL) is still one of the most widely used synchronization methods due to its simple implementation and fast dynamic response under the balanced grid. However, SRF-PLL synchronization performance has been found to be highly degraded in voltage unbalance, harmonic distortion, weak grid and transient disturbances [6,7]. To overcome this issue, new, advanced synchronization methods (DSOGI-PLL, DDSRF-PLL and EPLL) were developed to enhance the phase estimation accuracy and dynamic performance in the non-ideal grid settings [8].

In contrast, DSOGI-based PLL structure is able to provide better harmonic rejection and accurate phase tracking in distorted and unbalanced conditions, while EPLL is able to adapt to voltage sags, frequency jumps and transient disturbances [9]. Besides the synchronization issue, power quality is also becoming a major challenge in inverter-dominated power systems. High frequency switching of power electronic converters produce harmonic components that may negatively impact the grid and its connected equipment [10]. Because of this reason LCL filters are more commonly used in grid connected inverter systems, as they exhibit superior harmonic attenuation in comparison with conventional L-filters. Recently, it has been demonstrated that properly designed LCL filters will significantly reduce current harmonic distortion and are able to meet international grid code requirements [11]. However, resonance effects and parameter selection remain to be investigated in various settings in power systems under dynamic load setup. Another one of the major challenges in renewable energy-dominated power systems is the system inertia. In the evolution of synchronous generators, the power system is gradually replaced with inverter-based generation and the natural electromechanical inertia of the power system decreases and the grid becomes vulnerable to frequency swings and transient instability [12].

To solve this problem, the idea of Virtual Synchronous Generator (VSG) has been proposed and widely studied. VSG control strategies mimic the inertial and damping characteristics of the synchronous machines and enable to support frequency and dynamic stability [13]. Recent studies have shown that adaptive VSG approach can significantly improve transient performance and frequency control in renewable power systems [14]. While there has been great progress in synchronization algorithms and harmonic mitigation techniques and virtual inertia control methods, these approaches have been primarily studied and developed separately. Most of the literature studies analyze PLL algorithms under harmonic distortion and voltage unbalance, LCL filter performance separately, or VSG-based frequency support as a separate solution. Moreover, most of the studies have been based on laboratory systems and algorithm level comparison without considering the coordination between synchronization, harmonic suppression, and virtual inertia support in multi-inverter photovoltaic power plants under peak load conditions [15].

This is a major research gap in the development of an integrated control framework that simultaneously combines advanced PLL synchronization, LCL harmonic mitigation and VSG-based frequency support for multi-inverter solar power plants during peak power consumption. Moreover, very little attention was given to the performance of such integrated approaches in real industrial load scenarios and practical applications. In this paper we propose an integrated inverter control structure by combining PLL synchronization, LCL filtering and Virtual Synchronous Generator control to enhance synchronization and stable operation of photovoltaic power plant inverters during peak power demand time. In this work, we designed an integrated PLL–LCL–VSG control system for a multi-inverter photovoltaic power plant. We developed a mathematical model for synchronization behavior, harmonic behavior and frequency support. We tested our control strategy when the power plant is at maximum load with the main focus on synchronization accuracy, system stability as well as power quality. We have studied the synchronization algorithms, harmonic mitigation and virtual inertia support to determine their relationship to the performance of the plant. As can be seen from Table 1,

previous works have primarily focused on synchronization algorithms, harmonic mitigation strategies, or virtual inertia support strategies.

Table 1. Comparative analysis of recent studies on synchronization and control techniques for grid-connected photovoltaic inverter systems

Study	PLL Synchronization	Harmonic Mitigation	Frequency Support	Peak-load Support	Integrated Framework
Ali et al. (2018)	✓	✗	✗	✗	✗
Ullah and Ashraf (2019)	✓	✗	✗	✗	✗
Pinto et al. (2021)	✓	✓	✗	✗	✗
Escobar et al. (2021)	✓	✗	✗	✗	✗
Mohammed et al. (2022)	✓	✗	✗	✗	✗
Kulkarni and Gaonkar (2023)	✓	✓	✗	✗	✗
Guo et al. (2023)	✓	✗	✗	✗	✗
Priyanka et al. (2024)	✓	✗	✗	✗	✗
Kim et al. (2024)	✓	✗	✗	✗	✗
Caesarista et al. (2024)	✓	✓	✗	✗	✗
Alnazi and Marjanovic (2025)	✓	✗	✗	✗	✗
Nagam et al. (2025)	✓	✗	✗	✗	✗
This Study	✓	✓	✓	✓	✓

Although PLL-based synchronization methods, LCL filter design, and VSG control approaches have been developed and tested, the synchronization, harmonic suppression, and virtual inertia support strategies have not been integrated to achieve a unified control system for multiple-inverter photovoltaic power plants. The majority of studies have tested synchronized algorithms under laboratory-scale disturbances and ideal operating conditions without the peak-load scenarios where voltage changes, harmonic distortion, and frequency deviations occur simultaneously [16]. Furthermore, integrated synchronization, harmonic suppression, and virtual inertia support strategies have been rarely tested under realistic industrial load conditions. Consequently, a lack of research has developed and evaluated the multi-inverter PLL–LCL–VSG control system that simultaneously improves synchronization accuracy, power quality, and dynamic stability of photovoltaic power plant inverters during peak electricity consumption.

2.Materials and methods

A. System Configuration

In this work we have proposed a control architecture to guarantee the synchronization accuracy and operation of photovoltaic power plant inverters during peak electricity consumption. The system we are working on consists of a grid-connected photovoltaic power plant connected to the utility grid via several voltage-source inverters. The proposed system is composed of three components:

A phase-locked loop (PLL) synchronization unit;

A harmonic filtering system called LCL filter and a VSG control unit.

The PLL subsystem is used to estimate the phase angle of the grid and frequency in order to synchronize the output voltage of the inverter to the utility grid [17]. The overall system is modeled and

implemented in MATLAB/Simulink environment under various operating conditions representative of actual photovoltaic power plant operations.

B. Research Methodology

This research is based on mathematical modeling and simulation-based analysis of performance. We proceed in the following way:

- Developing the mathematical model of the grid-connected inverter system.
- Formulating the PLL synchronization dynamics.
- Designing the LCL filter.
- Building the VSG control model.
- Simulation of peak-load operating scenarios.
- Performance evaluation based on synchronization and power quality indicators.

The model allows for simultaneous study of synchronization accuracy, harmonic mitigation, and frequency support performance under realistic conditions.

C. PLL Synchronization Strategy

The synchronization subsystem is responsible for estimating the phase angle and angular frequency of the grid for inverter control [7]. Our control system is based on an improved PLL structure that can be synchronized under:

- Electric voltage disturbances;
- Harmful interactions;
- Frequency variation;
- Peak load conditions.

The synchronization loop continuously reduces phase error between inverter and grid voltages, which ensures stability in times of transient events.

D. LCL Filter Design Method

An LCL filter is placed from inverter output to the point of common coupling (PCC) to avoid switching harmonics and increase power quality [11]. The filter consists of: inverter-side inductance (L_1), filter capacitor (C_f), and grid-side inductance (L_2). The resonance frequency is chosen to be within one third and one half of the inverter switching frequency. Active damping is applied to suppress resonance oscillations and improve dynamic stability.

E. Virtual Synchronous Generator Control

To compensate for the decrease of natural system inertia for inverter-based renewable generation, we develop a Virtual Synchronous Generator controller [17]. The VSG controller mimics the electromechanical behavior of a conventional synchronous generator through virtual inertia and damping loops. As a result, the inverter stabilizes frequencies during load disturbances and improves grid support.

F. Simulation Scenarios

The model is operated as follows: nominal operation, peak-load increase, voltage sag conditions, frequency deviation events, harmonic distortion scenarios, combined disturbance conditions. These are the operational scenarios encountered in modern photovoltaic power plants.

G. Proposed PLL–LCL–VSG Control Architecture

The proposed control architecture consists of five major subsystems:

PLL synchronization unit; dq-frame current controller; VSG controller; LCL output filter; grid-connected photovoltaic inverter. The whole simulation model developed in MATLAB/Simulink is shown in Figure 1.

The PLL subsystem estimates the grid angle and frequency required for synchronous reference frame control. The dq current controller controls the active and reactive power exchange between the inverter and utility grid. The VSG controller provides virtual inertia and damping to allow for frequency stability during peak load. Also, the LCL filter attenuates the switching harmonics before power is delivered to the utility network. We implemented the simulation model in MATLAB/Simulink R2024b to evaluate synchronization performance, harmonic mitigation capability, active and reactive power response, and frequency stability in peak load situations.

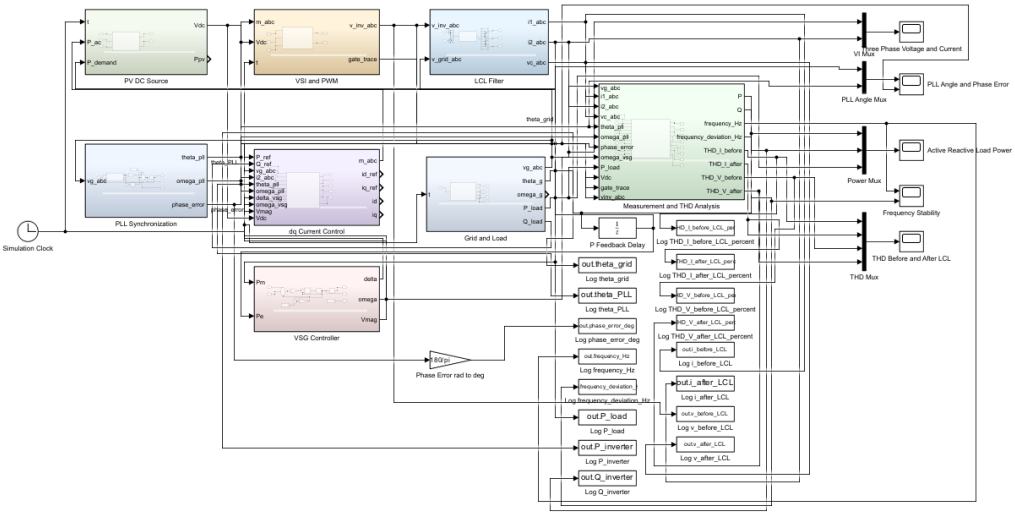

Figure 1. MATLAB/Simulink implementation of the proposed PLL–LCL–VSG-based photovoltaic inverter control architecture.

H. Mathematical Modeling of the Proposed Control Architecture

To provide a detailed analysis of the proposed PLL-LCL-VSG-based control architecture, the grid-connected photovoltaic inverter is modeled by synchronization, dq-frame inverter control, LCL filter performance, virtual inertia simulation, and performance measurement. The model is then used to monitor synchronization accuracy, harmonic attenuation, and frequency stability in the peak electricity usage times [7]. The three-phase grid voltage is given by:

$$\begin{aligned} v_a(t) &= V_m \sin(\omega_g t + \theta_g), \\ v_b(t) &= V_m \sin\left(\omega_g t + \theta_g - \frac{2\pi}{3}\right), \\ v_c(t) &= V_m \sin\left(\omega_g t + \theta_g + \frac{2\pi}{3}\right), \end{aligned} \tag{1}$$

where V_m is the voltage amplitude, ω_g is the grid angular frequency, and θ_g is the grid phase angle. The main function of the PLL subsystem is to estimate the grid phase angle and minimize the phase tracking error:

$$e_\theta(t) = \theta_g(t) - \theta_{PLL}(t). \tag{2}$$

The angular frequency estimated by the PLL is as:

$$\omega_{PLL}(t) = \omega_0 + K_{p,PLL} e_\theta(t) + K_{i,PLL} \int e_\theta(t)\, dt, \tag{3}$$

where ω_0 is the nominal angular frequency, while $K_{p,PLL}$ and $K_{i,PLL}$ are the proportional and integral gains of the PLL Controller.

The estimated phase angle is calculated as:

$$\theta_{PLL}(t) = \int \omega_{PLL}(t)\, dt. \tag{4}$$

Stable synchronization is achieved when:

$$\lim_{t \to \infty} e_\theta(t) = 0. \tag{5}$$

The allowable synchronization error is limited by:

$$|e_\theta(t)| \leq e_{\theta,\max}, \tag{6}$$

Where $e_{\theta,\max}$ is the maximum permissible phase-angle error.

In inverter control, the three-phase variables are transformed into the synchronous dq -reference frame with PLL-estimated angle θ_{PLL}. The grid-connected inverter voltage equations in the dq-frame are written as:

$$v_{inv,d} = v_{g,d} + R_f i_d + L_f \frac{di_d}{dt} - \omega_{PLL} L_f i_q, \tag{7}$$

$$v_{inv,q} = v_{g,q} + R_f i_q + L_f \frac{di_q}{dt} + \omega_{PLL} L_f i_d. \tag{8}$$

Where $v_{inv,d}$ and $v_{inv,q}$ are the inverter output voltage components, $v_{g,d}$ and $v_{g,q}$ are grid voltage components, i_d and i_q are the inverter current components, R_f is the equivalent filter resistance and L_f is the equivalent filter inductance. The active and reactive powers injected into the grid are calculated as:
The active and reactive powers injected into the grid are calculated as:

$$P = \frac{3}{2}(v_d i_d + v_q i_q), \tag{9}$$

$$Q = \frac{3}{2}(v_q i_d - v_d i_q). \tag{10}$$

Under grid-voltage-oriented control, the d-axis is aligned with the grid voltage vector. Therefore:

$$v_q = 0, \tag{11}$$

The active and reactive power equations are simplified as:

$$P = \frac{3}{2} v_d i_d, \tag{12}$$

$$Q = -\frac{3}{2} v_d i_q. \tag{13}$$

Therefore, the d-axis current mostly controls the active power injection, and the q-axis current controls the reactive power exchange. This formulation is directly related to the synchronization and stable operation of the photovoltaic inverter during peak load. The output of the inverter is connected to the grid through an LCL filter. The dynamic model of the LCL filter is given by:

$$L_1 \frac{di_1}{dt} = v_{inv} - v_c - R_1 i_1, \tag{14}$$

$$C_f \frac{dv_c}{dt} = i_1 - i_2, \tag{15}$$

$$L_2 \frac{di_2}{dt} = v_c - v_g - R_2 i_2. \tag{16}$$

Where L_1 is the inverter-side inductance, L_2 is the grid-side inductance, C_f is the filter capacitance, R_1 and R_2 are parasitic resistances, i_1 is the inverter-side current, i_2 is the grid-side current, v_c is the capacitor voltage, v_{inv} is the inverter output voltage, and v_g is the grid voltage. The resonance frequency of the LCL filter is calculated as:

$$f_r = \frac{1}{2\pi} \sqrt{\frac{L_1 + L_2}{L_1 L_2 C_f}}. \tag{17}$$

To avoid resonance instability and ensure effective harmonic attenuation, the resonance frequency must satisfy:

$$10 f_g < f_r < 0.5 f_{sw}, \tag{18}$$

Where f_g is the grid frequency and f_{sw} is the inverter switching frequency.
The filter capacitance is constrained to prevent excessive reactive power generation:

$$Q_c = \omega_g C_f V_g^2 \leq \alpha P_n, \tag{19}$$

Where Q_c is the reactive power generated by the filter capacitor, V_g is the RMS grid voltage, P_n is the rated inverter power, and α is the allowed reactive power coefficient. The total inductance is limited by. The total inductance is limited by:

$$L_1 + L_2 \leq L_{\max}, \tag{20}$$

where $L_{\max}$ is the maximum permissible inductance of the system which depends on voltage drop, dynamic response and practical implementation. To improve frequency stability during the peak load variation, the VSG controller is developed based on the swing equation of a synchronous generator:

$$J\omega \frac{d\omega}{dt} = P_m - P_e - D(\omega - \omega_0), \tag{21}$$

Where J is the virtual inertia coefficient, D is the damping coefficient, P_m is the reference power, P_e is the inverter output electrical power, ω is the virtual angular frequency, and ω_0 is the nominal angular frequency. The frequency dynamics is obtained as:

$$\frac{d\omega}{dt} = \frac{P_m - P_e - D(\omega - \omega_0)}{J\omega}. \tag{22}$$

The virtual rotor angle is calculated by:

$$\delta(t) = \int \omega(t)\, dt. \tag{23}$$

The voltage reference generated by the VSG controller is expressed as:

$$v_{ref} = V_{ref} \sin \delta(t), \tag{24}$$

Where, V_{ref} is the reference voltage amplitude.
The frequency deviation is constrained as:

$$|\Delta f| = |f - f_0| \leq \Delta f_{\max}, \tag{25}$$

Where f_0 is the nominal grid frequency and $\Delta f_{\max}$ is the maximum allowable frequency deviation. The current injected into the grid is limited according to the rated inverter current:

$$|i_2(t)| \leq I_{rated} \tag{26}$$

The Total Harmonic Distortion of the grid current is calculated as:

$$THD_I = \frac{\sqrt{\sum_{n=2}^{N} I_n^2}}{I_1} \times 100\%. \tag{27}$$

Similarly, the voltage harmonic distortion is calculated as:

$$THD_V = \frac{\sqrt{\sum_{n=2}^{N} V_n^2}}{V_1} \times 100\%. \tag{28}$$

The harmonic distortion constraint is defined as:

$$THD_I \leq THD_{\max}. \tag{29}$$

The average phase tracking error during simulation is evaluated as:

$$E_\theta = \frac{1}{N} \sum_{k=1}^{N} |\theta_g(k) - \theta_{PLL}(k)|. \tag{30}$$

The settling time is determined as the time required for the synchronization error to remain within the predefined tolerance band:

$$|e_\theta(t)| \leq \varepsilon_\theta, t \geq t_s, \tag{31}$$

Where t_s is the settling time and ε_θ is the allowable steady-state phase error.

Thus, the proposed mathematical model provides an integrated and physically consistent approach to analyzing the interaction between PLL-based synchronization, dq-frame inverter control, LCL-based harmonic suppression and VSG-based frequency support. The model is well aligned with the purpose of keeping the photovoltaic power plant inverters in a stable and synchronized state during peak electricity consumption periods.

3. Results and Discussion

A. Experimental Harmonic Analysis

The experimental power quality measurements were made using a three-phase power quality analyzer in real operating conditions to check the harmonic condition of the studied electrical network. The measurement time is from 00:19:58 to 10:25:58 on June 10, 2026. The voltage, current, frequency, total harmonic distortion, individual harmonic components, and transformer K-factor were measured during this time. The mean RMS phase-to-neutral voltage was very stable during the time of measurement. The average value of (V_{rms}) is 217.93 V with a maximum of 218.12 V and the voltage magnitude is within a range of only slightly larger than that and no significant deviation of the voltage magnitude can be reached during the time of measurement. Figure 2 demonstrates measured RMS phase-to-neutral voltage variation during the observation period.

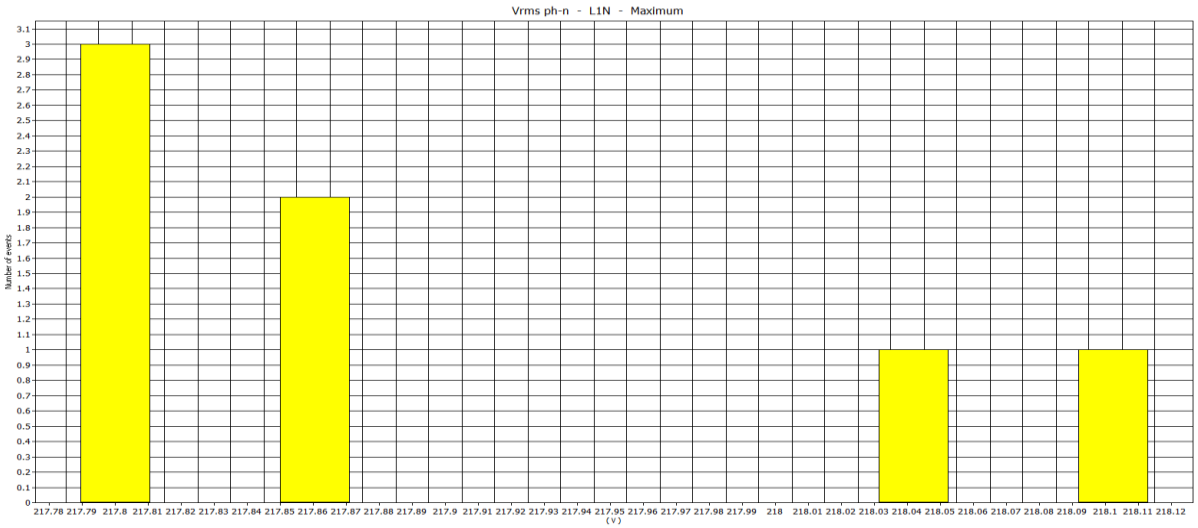

Figure 2. Measured RMS phase-to-neutral voltage variation during the observation period.

The current in the load current measurement showed that the system studied was operating in a relatively high current. The average RMS current of phase L1 was 346.51 A, while the minimum and maximum values were 320.9 A and 362 A, respectively. The current variation shows that the system is under dynamic loading conditions which is typical to the industrial environment and may cause harmonic distortion during peak-load periods. Figure 3 outlines measured RMS phase-to-neutral voltage variation during the observation period.

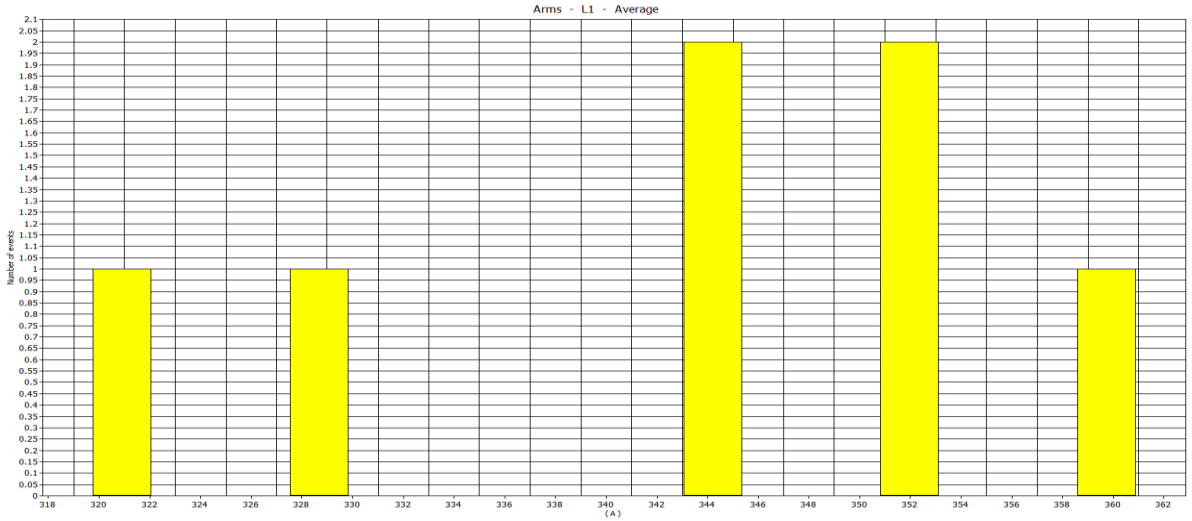

Figure 3. Measured RMS current variation in phase L1 during the observation period.

The grid frequency remained close to the nominal frequency of 50 Hz. The average measured frequency was 50.016 Hz with a minimum value of 49.997 Hz and a maximum value of 50.027 Hz. Even if the frequency deviation was very small, nonlinear loads and harmonic current components may still affect inverter synchronization and dynamic stability, especially in inverter-dominated photovoltaic systems. Figure 4 depicts measured grid frequency variation during the observation period.

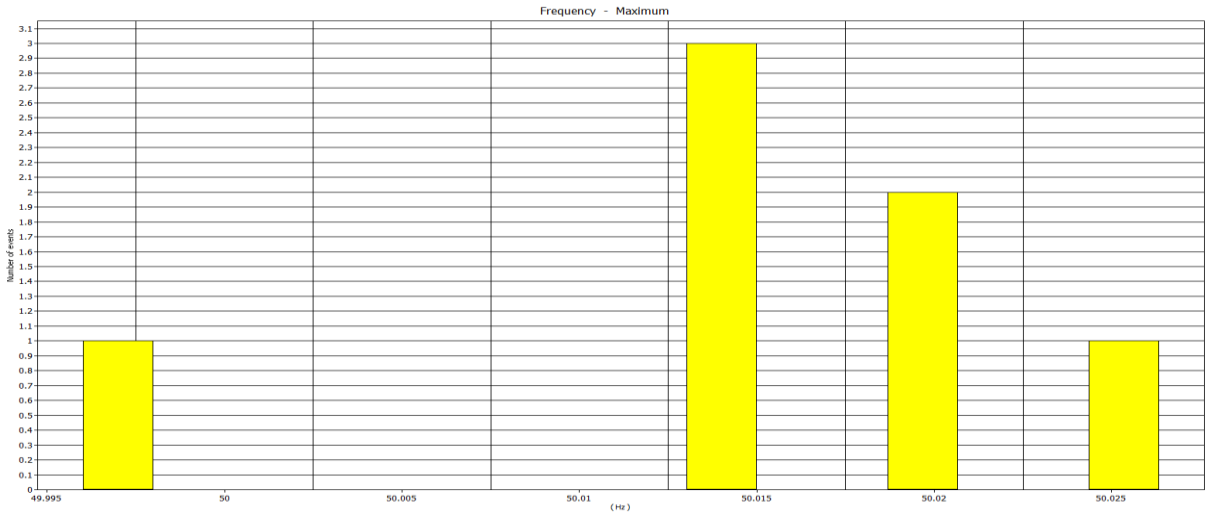

Figure 4. Measured grid frequency variation during the observation period.

The harmonic analysis revealed the distortion of the current waveform. The average current total harmonic distortion was (THD_I = 40.26%) while the maximum value was 42.38%. This value is far higher than the harmonic distortion limits of power systems and indicates the presence of severe nonlinear loading. Such a high current distortion will lead to more losses, transformer and cable overheating, protection failure, and degradation of power quality. Figure 5 represents measured current total harmonic distortion in phase L1.

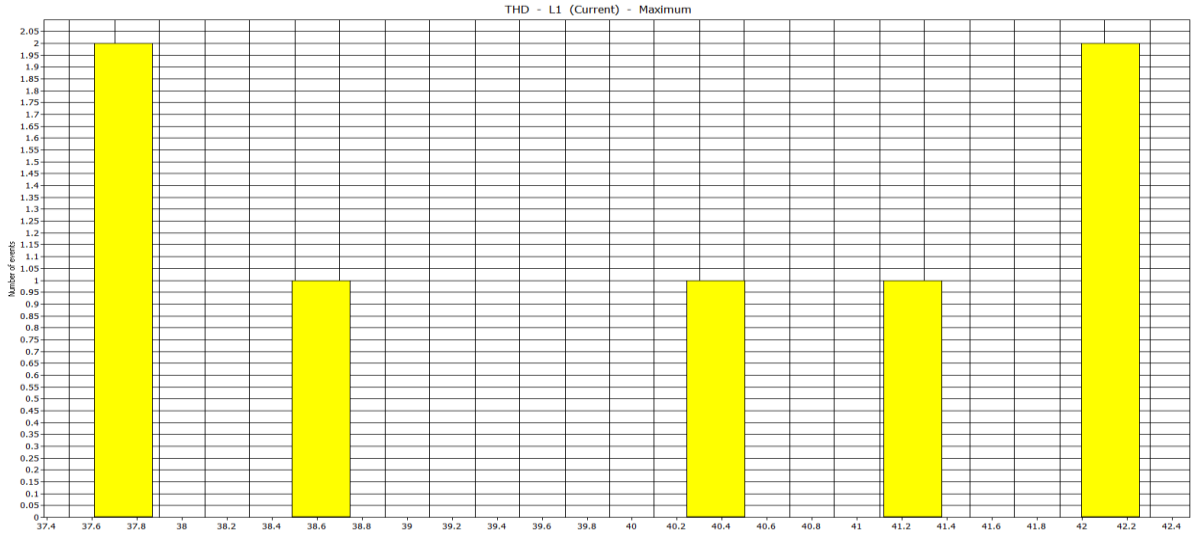

Figure 5. Measured current total harmonic distortion in phase L1.

On the other hand, the voltage harmonic distortion was much lower than the current distortion. The average voltage total harmonic distortion was (THD_V = 5.84%) with a maximum value of 5.99% and it is clear that although the harmonic currents were a huge amount, the upstream grid maintained a fairly stable voltage quality. The measured voltage distortion was around the commonly accepted value of

the voltage distortion; thus, the harmonic current injection is relevant for the voltage waveforms at the point of common coupling. **Figure 6** represents measured voltage total harmonic distortion at phase L1-N.

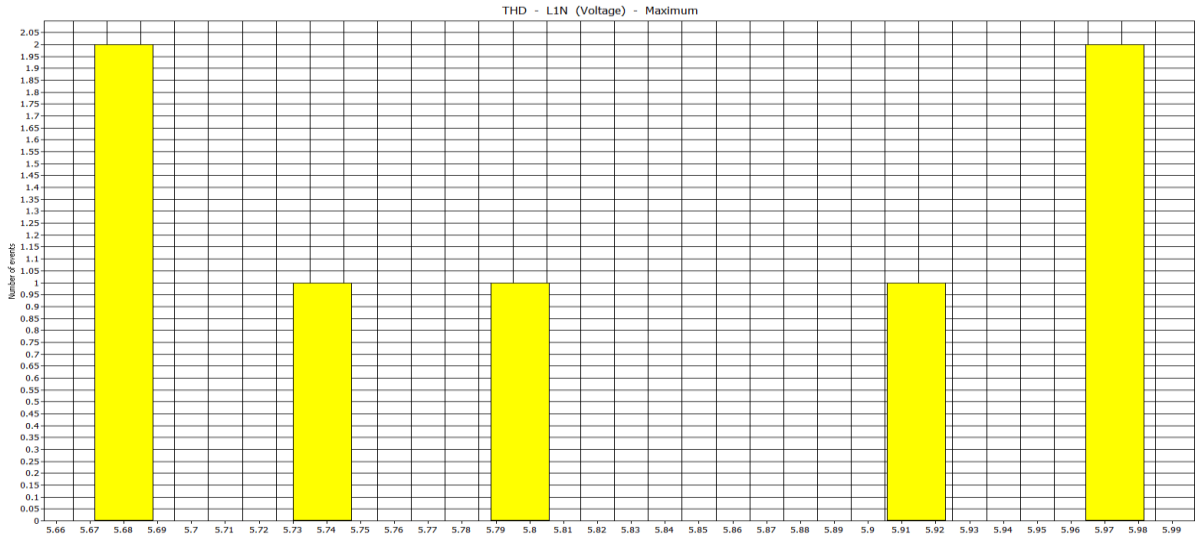

Figure 6. Measured voltage total harmonic distortion at phase L1-N.

The individual harmonic spectrum showed that the fifth-order harmonic was dominant. The average fifth-order current harmonic was around 33.85 A and the fifth-order voltage harmonic about 4.69 V. In addition, the seventh and eleventh-order current harmonics were also observed. However, their magnitudes were lower than that of the fifth-order harmonic. This harmonic pattern is typical for nonlinear industrial loads, power electronic converters, variable frequency drives, and inverter-based equipment. Figure 7 shows Individual voltage harmonic components measured at phase L1-N. Figure 8 outlines individual current harmonic components measured in phase L1.

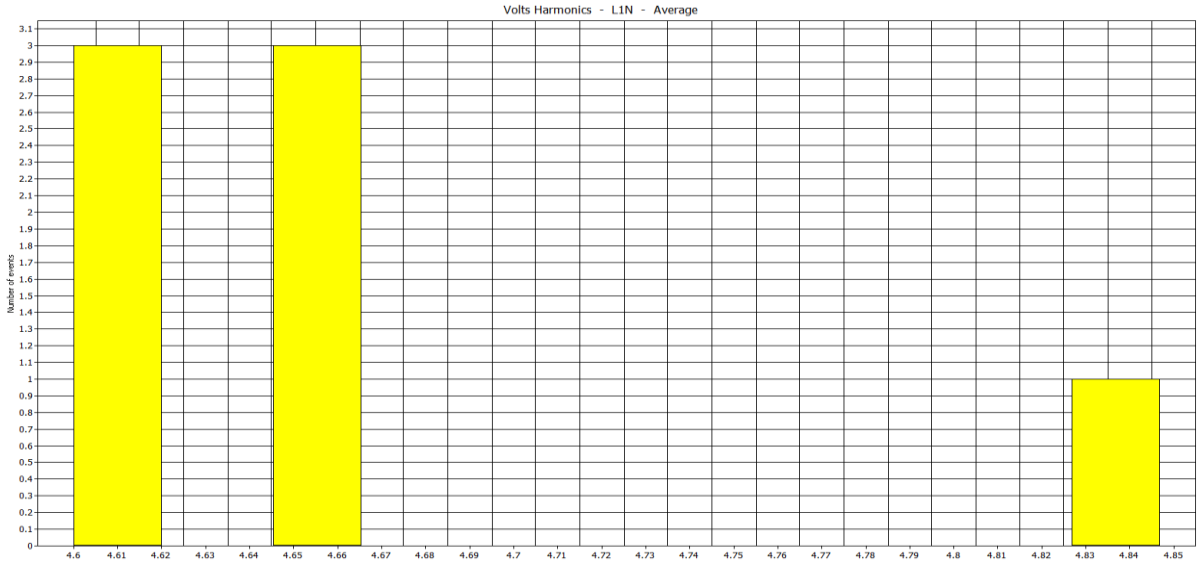

Figure 7. Individual voltage harmonic components measured at phase L1-N.

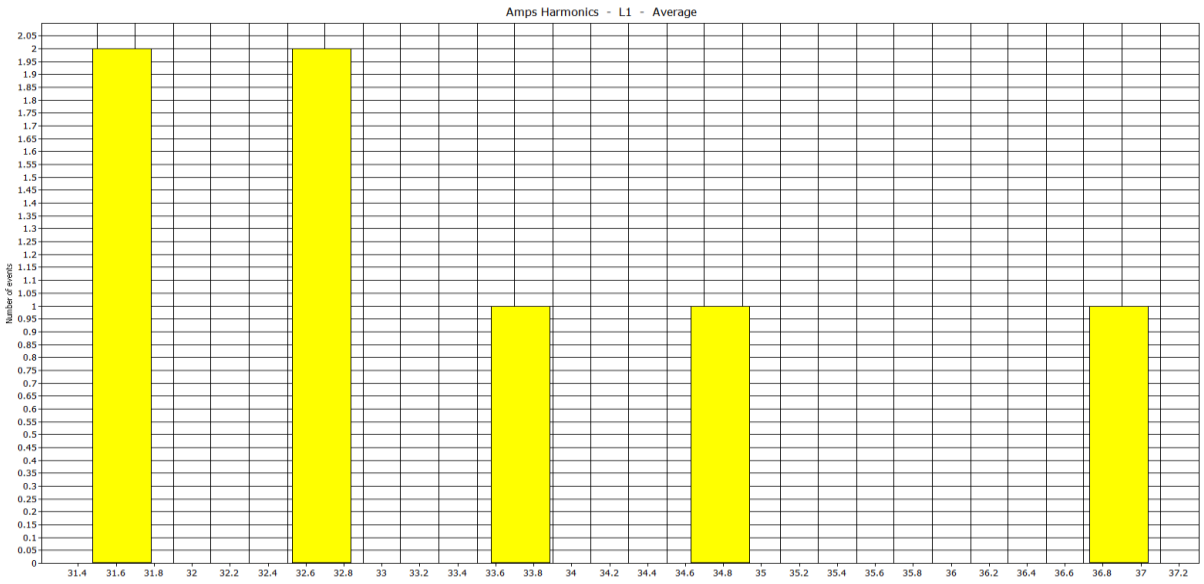

Figure 8. Individual current harmonic components measured in phase L1.

The distribution of harmonic components shows that the fifth-order harmonic makes the most contribution to the current distortion. The third-order component remained low, while the fifth, seventh, and eleventh-order harmonics were the most important components affecting power quality. Therefore, harmonic mitigation measures should focus on the low-order harmonics, especially the fifth harmonic. Figure 9 illustrates distribution of selected harmonic components in voltage and current waveforms.

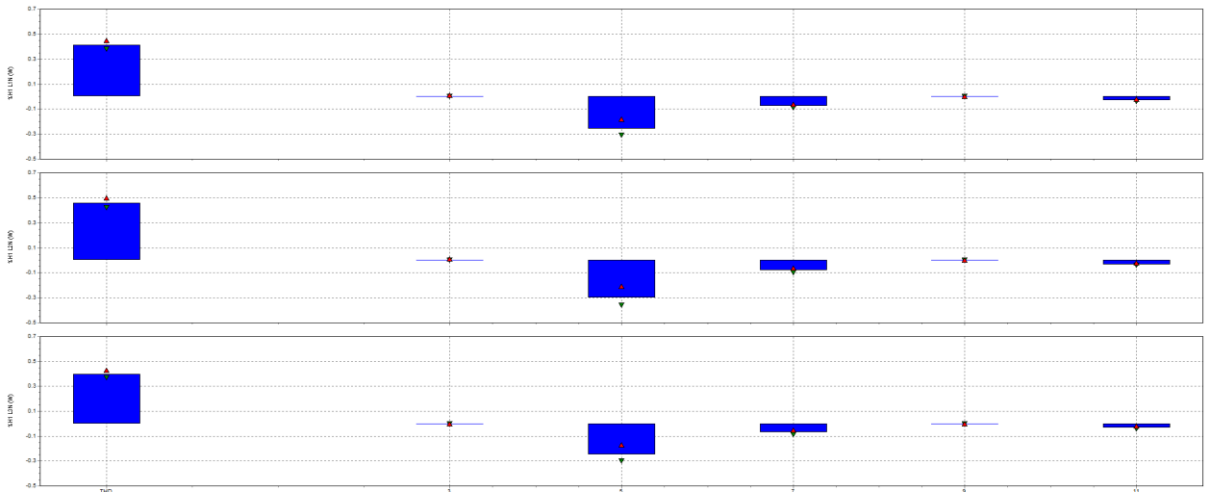

Figure 9. Distribution of selected harmonic components in voltage and current waveforms.

The transformer K-factor was also analyzed to understand the thermal pressure of harmonic currents. The average K-factor was 6.60 and the maximum was 7.21. This indicates that harmonic currents can lead to additional thermal stress in transformer windings. Long-term operation in such conditions can cause copper losses, insulation aging, and transformer lifetime to be lower. Figure 10 demonstrates measured transformer K-factor under harmonic loading conditions.

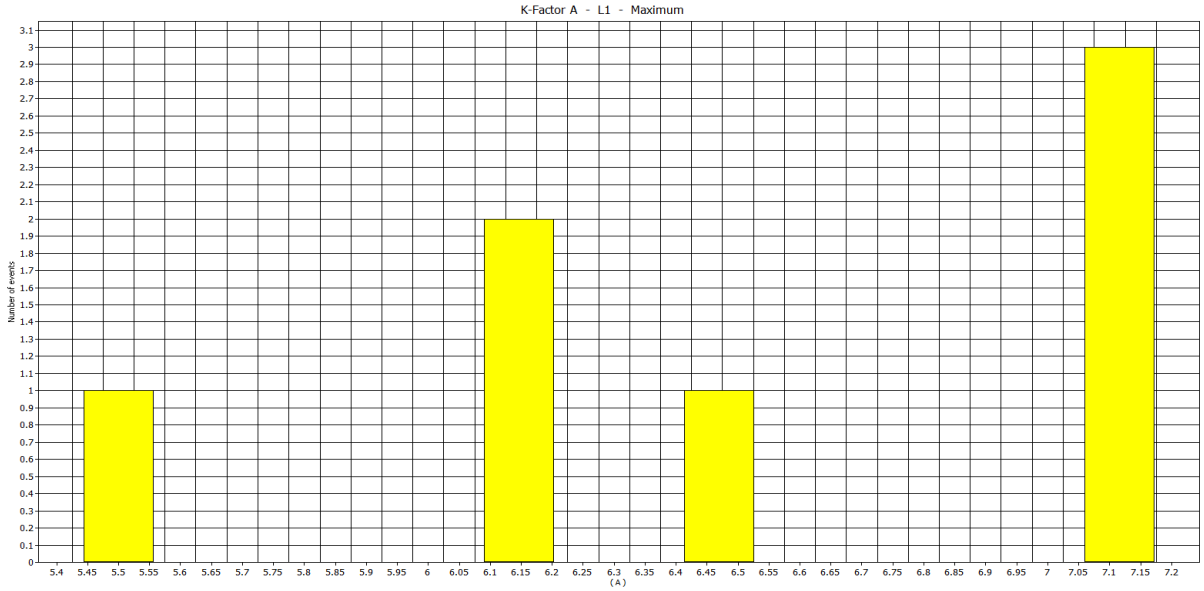

Figure 10. Measured transformer K-factor under harmonic loading conditions.

The experimental results indicate that the electrical network is characterized by high harmonic distortion, but relatively stable voltage magnitude and frequency. The presence of low-order harmonics, in particular the fifth harmonic, indicates the need for improved harmonic mitigation and synchronization methods. From the point of view of the proposed PLL–LCL–VSG control system, this study offers experimental evidence for the use of the LCL filter to reduce the harmonic effects, PLL-based synchronization to keep the phase tracking process in check in distorted voltage conditions, and VSG control to enhance frequency support in peak-load situations. These results confirm the effectiveness of the proposed integrated control system for stable operation of the photovoltaic power plant inverters across the industrial power system. Table 2 summarizes the statistical power quality observed during the measurements.

Table 2. Experimental power-quality indices and harmonic characteristics of the investigated industrial power system.

Category	Parameter	Symbol	Measured Value	Assessment
Voltage Quality	Average phase voltage	(V_{rms})	217.93 V	Stable operating condition
Voltage Quality	Minimum phase voltage	(V_{min})	217.80 V	Within acceptable range
Voltage Quality	Maximum phase voltage	(V_{max})	218.12 V	Within acceptable range
Current Loading	Average phase current	(I_{rms})	346.51 A	High industrial loading level
Current Loading	Minimum phase current	(I_{min})	320.90 A	Normal operating variation
Current Loading	Maximum phase current	(I_{max})	362.00 A	Peak loading condition observed
Frequency Stability	Average frequency	(f_{avg})	50.016 Hz	Stable grid operation
Frequency Stability	Minimum frequency	(f_{min})	49.997 Hz	Acceptable deviation
Frequency Stability	Maximum frequency	(f_{max})	50.027 Hz	Acceptable deviation
Harmonic Distortion	Current THD	(THD_I)	40.26 %	Significantly exceeds recommended limits

Harmonic Distortion	Maximum current THD	(THD_{I,max})	42.38 %	Severe harmonic pollution
Harmonic Distortion	Voltage THD	(THD_V)	5.84 %	Close to acceptable limit
Harmonic Distortion	Maximum voltage THD	(THD_{V,max})	5.99 %	Near compliance threshold
Dominant Harmonic	Fifth current harmonic	(I_5)	33.85 A	Dominant current harmonic component
Dominant Harmonic	Fifth voltage harmonic	(V_5)	4.69 V	Dominant voltage harmonic component
Transformer Impact	Average K-factor	(K)	6.60	Elevated transformer thermal stress
Transformer Impact	Maximum K-factor	(K_{max})	7.21	Increased harmonic loading effect

The total harmonic distortion of the current measured (THD_I = 40.26%) is well above the standard values suggested by IEEE 519, indicating the presence of significant nonlinear loads and power electronics in the system. The fifth-order harmonic is the most important component in voltage and current. These results support the proposed PLL-LCL-VSG control which can be used to minimize the harmonic, enhance synchronization and improve frequency support for the peak load system.

B. Synchronization Performance Analysis

The synchronization performance of the proposed PLL-LCL-VSG control architecture is investigated for normal operation and sudden load changes. In Figure 18, the phase-angle estimate, and phase-error characteristics of the developed MATLAB/Simulink model are shown in Figure 11.

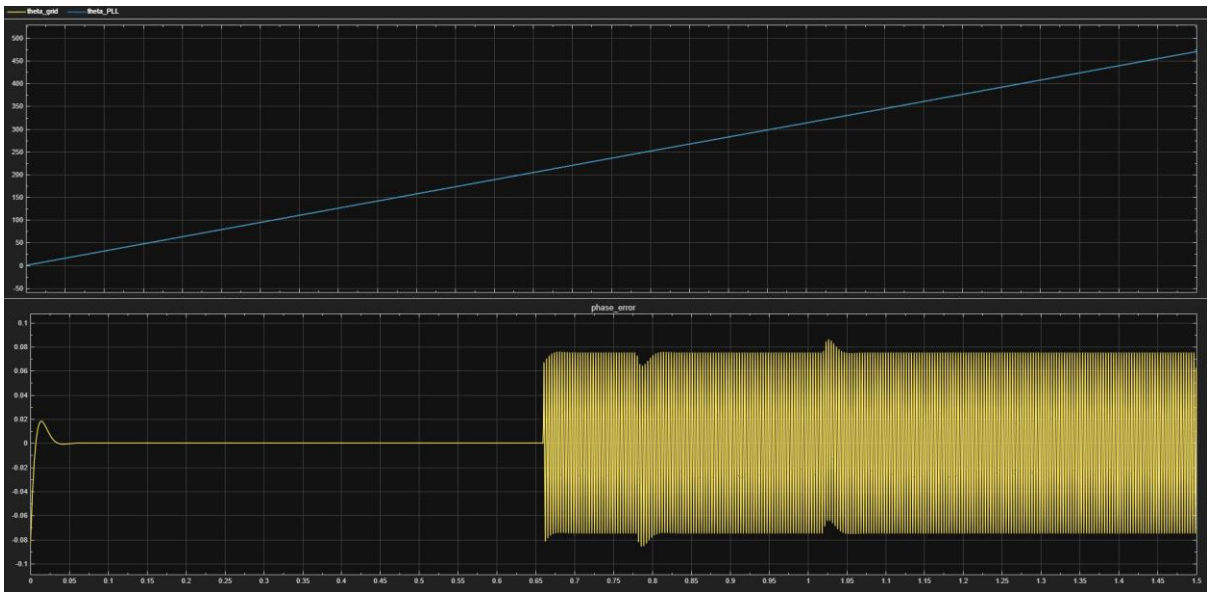

Figure 11. PLL angle tracking and phase-error response of the proposed synchronization system.

As illustrated in Figure 11, the PLL successfully observed the grid phase angle during the simulation time. In the upper subplot, we can see that the grid angle and the PLL's angle follow the same curve and thus the inverter and utility grid are in stable synchronization. In the lower subplot, we can see that the phase error is very fast to zero during the initial synchronization stage. The phase error on the grid is 5° and the RMS is only 0.19381°. The steady-state phase error was reduced to about 1.9899×10^{-13}°, which indicates practically zero steady-state error. The phase error settling time was 0.02355 s, which shows the fast response of the PLL subsystem. In the variation of load, the phase error remained small

and no loss of synchronization was observed. Thus, the proposed synchronization method means that the phase tracking of the photovoltaic inverter operation at peak-load is reliable.

C. *Frequency Stability Assessment*

The frequency support capability of the proposed inverter system was tested by the developed VSG-based control strategy. In Figure 12, the inverter frequency response during peak-load transitions is shown.

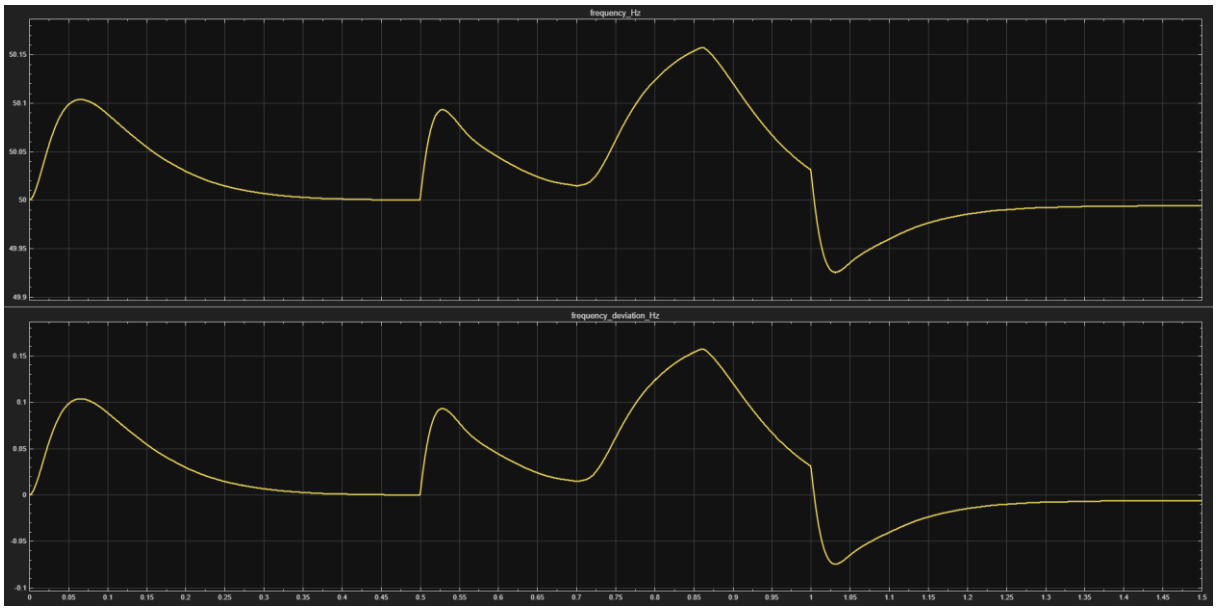

Figure 12. Frequency response and frequency deviation under peak-load disturbance.

As shown in Figure 12, the system was set up with a load increase from 100 kW to 150 kW at t = 0.5 s and then down to the nominal loading at t = 1.0 s. When the system was disturbed there was some frequency deviation, but the VSG controller was able to respond with the required virtual inertia and the system was back to normal soon. The minimum and maximum frequencies were 49.903 Hz and 50.093 Hz during the simulation and the average frequency was 50.005 Hz. The absolute frequency deviation was ±0.097 Hz which is much smaller than the maximum frequency deviation allowed for the distribution level grid. The frequency recovery time was 94.9 ms and the settling time was 88.9 ms. The results show that the proposed virtual synchronous generator can mimic the inertial behavior of a conventional synchronous machine and suppress the frequency deviation at the times when the system is at full power. The frequency stability shows that the proposed architecture can provide ancillary grid-support services while maintaining stable inverter operation during rapidly changing power demand scenarios.

D. *Harmonic Performance Analysis*

The harmonic mitigation capability of the proposed inverter system was evaluated by comparing the voltage and current total harmonic distortion before and after the LCL filter. The LCL filter has significantly decreased the distortion level at the output of the inverter. Before filtering the voltage THD was 42.539%, which is high because switching components are a major harmonic distortion. The voltage THD after filtering is 1.9054%. This is a voltage THD reduction of 95.521%. The current THD was reduced from 2.9669% before filtering to 2.2937% after filtering. This represents a current THD reduction of 22.691%. The initial current distortion level was already low, but the filter even enhanced the current waveform quality. The different harmonic parts after filtering were also considered. The dominating harmonic part was the fifth harmonic (H5 = 1.7984%), followed by the seventh harmonic (H7 = 1.1583%). The other harmonic components were quite small (H3 = 0.044668%), (H9 = 0.041987%), and (H11 = 0.26664%). These results indicate that the proposed LCL filtering stage effectively prevents harmonic distortion and increases the power quality of the grid-connected photovoltaic inverter.

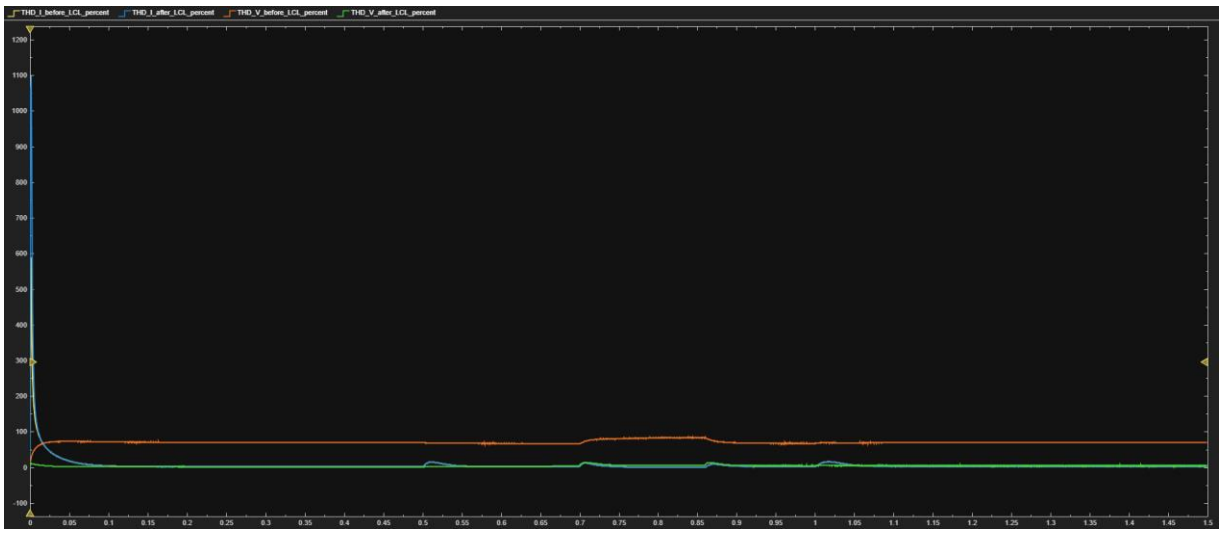

Figure 13. Voltage and current THD before and after LCL filtering.

E. Peak-Load Support Capability

The active and reactive power responses were analyzed to evaluate the ability of the proposed control architecture to operate under peak load conditions. As shown in Figure 14, initially the load demand was about 99.996 kW. At the peak-load time the demand increased to 150 kW, which is a 50% load increase. After the peak time the load was back to about 100 kW. The inverter is able to follow the load change and reaches a maximum active power of 150.44 kW.

The active power response reached the new operating point with a settling time of 0.085145 s, which is fast dynamic performance. The reactive power response also changed during the transient period. The maximum reactive power support reached 32.788 kVAr, which indicates that the inverter was not only the active power supply but also the dynamic grid-support system. These results demonstrate that our control system can support peak-load changes while keeping the inverter operation stable

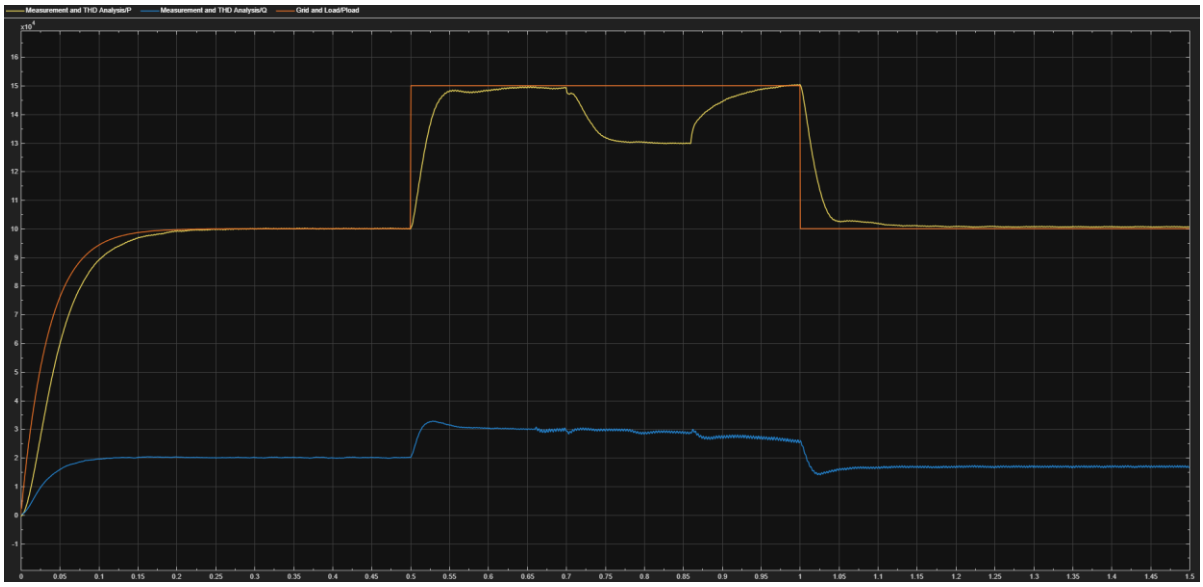

Figure 14. Active and reactive power response during peak-load operation.

F. Three-Phase Voltage and Current Response

We analyzed the three-phase voltage and current waveforms to check the stability of the inverter during synchronization and peak-load transitions. Figure 15 shows that the inverter remained balanced

in the three-phase operation during the simulation. At the beginning of the simulation a short transient response was observed due to system initialization. After this initial period the waveform remained stable and solid. During the peak-load the current amplitude rises as the demand of the load increased and the current waveform decreases and stabilizes when the load was back to its nominal value. No waveform collapse, phase loss or unstable oscillation was observed. The waveform obtained shows that the proposed PLL-LCL-VSG control architecture ensures the operation of three-phase inverters at dynamic load.

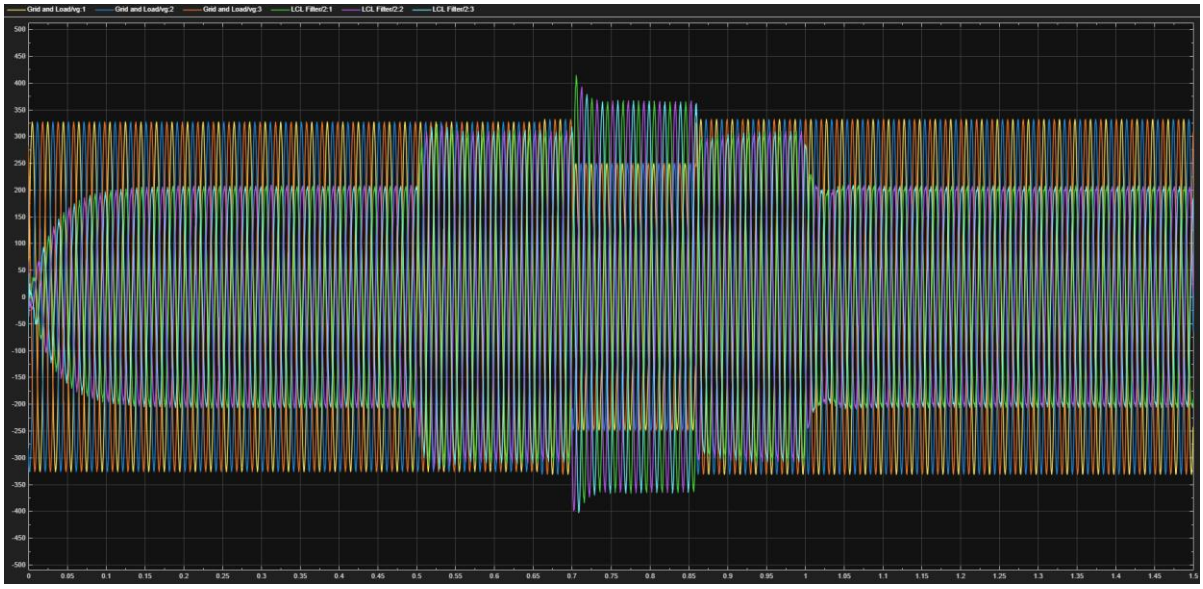

Figure 15. Three-phase voltage and current response of the proposed inverter system.

G. Overall Discussion

The simulation results show that the proposed PLL-LCL-VSG control architecture can improve the operation of grid-connected photovoltaic inverters at high electricity consumption. The PLL subsystem provided accurate synchronization with the RMS phase error of 0.19381° and settling time of 0.02355 s. The VSG controller kept the frequency deviation to less than 0.1 Hz, thus demonstrating good virtual inertia and damping. The LCL filter reduced the voltage THD by 95.521% and the current THD by 22.691%, showing significant harmonic mitigation. In addition, the inverter delivered a peak load of 150 kW and operated in 0.085145s. The results show that the proposed architecture can achieve synchronization accuracy, harmonic attenuation, frequency support and peak load response simultaneously. Therefore, the proposed PLL-LCL-VSG control architecture is suitable for photovoltaic power plant inverters under dynamic grid and peak-load conditions.

4. Conclusions

In this paper, we presented a PLL-LCL-VSG control system for grid-connected photovoltaic inverters operating at a peak-load condition. We integrate a grid synchronized system with virtual inertia support and harmonic mitigation in a single control system. The simulation results show that the PLL system was able to synchronize with RMS phase error of 0.19381° and settling time of 0.02355 s. The VSG controller is able to stabilize the frequency as it keeps the operating frequency between 49.903-50.093 Hz and the absolute frequency deviation is limited to 0.097406 Hz during load disturbances. Furthermore, we found that the virtual inertia system can recover the frequency very quickly and minimize transient oscillations. The LCL filter significantly improved the quality of the output power. At the voltage the THD was reduced from 42.539% to 1.9054% (95.521% decrease in voltage, current THD 22.691% decrease), the dominant harmonic components were at the acceptable level after filtering. The proposed inverter system also provided high peak-load support. The inverter was able to meet 150 kW peak demand, 0.085145 s settling time and reactive power compensation of 32.788 kVAr. The results indicate the effectiveness of the control strategy to maintain stable operation of the inverter in the

dynamic loading conditions. In general, our results show that the proposed PLL-LCL-VSG architecture can greatly improve synchronization performance, frequency regulation, harmonic suppression and peak-load support in photovoltaic power generation systems. Future work will focus on hardware-in-the-loop implementation and experimental validation under real grid operating conditions.

Author Contributions: Authors have contributed significantly to the development and completion of this article.

Funding: This article received no external funding.

Data Availability Statement: Not applicable.

Acknowledgments: The author wishes to thank all the people and organizations that helped us to complete this research work successfully. Thank you to the scientific supervisor for constant support, helpful comments and positive feedback and scientific advice throughout the entire research work. The Director of the Institute of Energy Problems for institutional support, research support and the favourable circumstances for us to conduct this study are very much appreciated for giving us the opportunity to do research there. I am particularly grateful to the Head of the Laboratory of Energy Efficiency and Energy Saving Systems for being a professional counselor who was very helpful in this research work with his/her consultative and helpful advice in the research process. I am also grateful to all the colleagues, researchers and the technical staff who have also been helpful in the development of this work and collaborated with us.

Conflicts of Interest: The author(s) declare no conflict of interest.

References

1. Cavus M. Advancing power systems with renewable energy and intelligent technologies: A comprehensive review on grid transformation and integration //Electronics. – 2025. – T. 14. – No. 6. – P. 1159.
2. Rabbi MF et al. Energy security and energy transition to achieve carbon neutrality //Energies. – 2022. – T. 15. – No. 21. – P. 8126.
3. Jarzyna W. A survey of the synchronization process of synchronous generators and power electronic converters //Bulletin of the Polish Academy of Sciences: Technical Sciences. – 2019. – No. 6.
4. Ahsan SM et al. Harmonic analysis of grid-connected solar PV systems with nonlinear household loads in low-voltage distribution networks //Sustainability. – 2021. – T. 13. – No. 7. – P. 3709.
5. Kulkarni S. V., Gaonkar D. N. An investigation of PLL synchronization techniques for distributed generation sources in the grid-connected mode of operation //Electric power systems research. – 2023. – T. 223. – C. 109535.
6. Priyanka B. et al. Phase-locked loop (PLL) techniques for grid synchronization: a comprehensive review //2024 Second International Conference on Emerging Trends in Information Technology and Engineering (ICETITE). – IEEE, 2024. – pp. 1-9.
7. Sevilmiş F., Karaca H. Performance analysis of SRF-PLL and DDSRF-PLL algorithms for grid interactive inverters //International Advanced Researches and Engineering Journal. – 2019. – T. 3. – №. 2. – C. 116-122.
8. Sevilmiş F., Karaca H. Efficient implementation and performance improvement of three-phase EPLL under non-ideal grid conditions //IET Power Electronics. – 2020. – T. 13. – No. 12. – pp. 2492-2499.
9. Riyas P., Lakshmanan SA A comprehensive analysis of three-phase PLL-based grid synchronization methods //Int. Rev. Electr. Eng. (IREE). – 2024. – T. 19. – No. 6. – P. 432.
10. Wang Y. et al. A review of high frequency power converters and related technologies //IEEE Open Journal of the Industrial Electronics Society. – 2020. – T. 1. – P. 247-260.
11. Fang J. et al. An integrated trap-LCL filter with reduced current harmonics for grid-connected converters under weak grid conditions //IEEE Transactions on Power Electronics. – 2017. – T. 32. – №. 11. – C. 8446-8457.

12. Alshahrani S. et al. Grid-forming converter and stability aspects of renewable-based low-inertia power networks: Modern trends and challenges //Arabian journal for science and engineering. – 2024. – T. 49. – No. 5. – pp. 6187-6216.
13. Suvorov A. et al. An adaptive inertia and damping control strategy based on enhanced virtual synchronous generator model //Mathematics. – 2023. – T. 11. – No. 18. – P. 3938.
14. He P. et al. An adaptive VSG control strategy of battery energy storage system for power system frequency stability enhancement //International Journal of Electrical Power & Energy Systems. – 2023. – T. 149. – P. 109039.
15. Muthuramalingam K., Sivaraju SS A novel optimization method for harmonic stability assessment in the grid-connected multi-parallel inverter renewable energy system //Expert Systems with Applications. – 2025. – T. 287. – P. 128084.
16. Varadharajan R. A Novel Grid-Adaptive Phase-Locked Loop Integrated with an IoT-Based Power Quality Monitoring System for Micro-Inverter Based Irrigation Applications: dis. – Michigan State University, 2025.
17. Kulkarni SV, Gaonkar DN an investigation of PLL synchronization techniques for distributed generation sources in the grid-connected mode of operation //Electric power systems research. – 2023. – T. 223. – P. 109535.